Multi-scroll hidden attractors with two stable equilibrium points

Cite as: Chaos **29**, 093112 (2019); https://doi.org/10.1063/1.5116732
Submitted: 27 June 2019 . Accepted: 23 August 2019 . Published Online: 10 September 2019

Quanli Deng, and Chunhua Wang

Chaos ARTICLE scitation.org/journal/cha

Multi-scroll hidden attractors with two stable equilibrium points

Cite as: Chaos **29**, 093112 (2019); doi: 10.1063/1.5116732
Submitted: 27 June 2019 · Accepted: 23 August 2019 ·
Published Online: 10 September 2019

Quanli Deng[a] and Chunhua Wang[b]

AFFILIATIONS

College of Computer Science and Electronic Engineering, Hunan University, Changsha 410082, China

[a]**E-mail:** quanliden@hnu.edu.cn
[b]**Author to whom correspondence should be addressed:** wch1227164@hnu.edu.cn

ABSTRACT

Multiscroll hidden attractors have attracted extensive research interest in recent years. However, the previously reported multiscroll hidden attractors belong to only one category of hidden attractors, namely, the hidden attractors without equilibrium points. Up to now, multiscroll hidden attractors with stable equilibrium points have not been reported. This paper proposes a multiscroll chaotic system with two equilibrium points. The number of scrolls can be increased by adding breakpoints of a nonlinear function. Moreover, the two equilibrium points are stable node-foci equilibrium points. According to the classification of hidden attractors, the multiscroll attractors generated by a novel system are the hidden attractors with stable equilibrium points. The dynamical characteristics of the novel system are studied using the spectrum of Lyapunov exponents, a bifurcation diagram, and a Poincaré map. Furthermore, the novel system is implemented by electronic circuits. The hardware experiment results are consistent with the numerical simulations.

Since the first hidden attractor was found in Chua's circuit, hidden attractors have received great interest. The chaotic attractors generated by systems with no equilibrium point, infinite equilibrium points, and only stable equilibrium points are hidden attractors. The Shilnikov criteria cannot be used to verify the existence of the hidden attractors. Recently, constructing hidden attractors with multiscroll, which have more complicated dynamical properties, is a hot topic. However, the previously reported multiscroll hidden attractors belong to only one category of hidden attractors, namely, hidden attractors without equilibrium points. In this paper, we construct a novel chaotic system with multiscroll hidden attractors, which has two equilibrium points. The number of scrolls can be increased by adding breakpoints of the piecewise linear function. Moreover, the two equilibrium points are stable node-foci equilibrium points. According to the classification of hidden attractors, the multiscroll attractors generated by the novel system are the hidden attractors with only stable equilibrium points.

I. INTRODUCTION

In the past few decades, the study of chaotic systems has been greatly developed both in applications and in theories. Chaotic systems have been applied to secure the communication,[1] image encryption,[2,3] neural networks,[4] and so on. Therefore, it is of great significance to study chaotic systems. The equilibrium points of chaotic systems play an important role in the chaotic theory. It was thought that chaotic attractors are closely related to the equilibrium points of chaotic systems. According to the Shilnikov criteria,[5] the emergence of chaos requires at least one unstable equilibrium point, and an attractor can be derived from an unstable equilibrium point. Constructing chaotic systems with complex dynamical characteristics has always been the focus of this research. Multiscroll chaotic systems provoked extensive researches for their more complex dynamical characteristics than single-scroll ones. The first multiscroll oscillator[6] was derived from the original Chua's circuit by introducing a nonlinear resistor with multiple breakpoints. Then, various nonlinear functions such as stair function,[7] saw-tooth function,[8] piecewise linear function,[9] and so on were used to construct multiscroll chaotic systems. The basic idea of constructing a multiscroll chaotic system is to use a nonlinear function with multiple breakpoints to increase the number of unstable equilibrium points, so as to generate scrolls from the extra equilibrium points.

However, the discovery of hidden attractors posed a challenge to apply the conventional Shilnikov criteria to verify chaos. An attractor is called a hidden attractor if its attraction basin does not intersect

with small neighborhoods of any equilibrium point; otherwise, it is called a self-excited attractor.[10] According to the definition of hidden attractors, hidden chaotic attractors are not generated from the equilibrium points of a chaotic system. Therefore, the Shilnikov criteria cannot be used to verify hidden attractors. From a computational perspective, hidden attractors can be classified into three categories: hidden attractors with stable equilibrium points, hidden attractors without equilibrium points, and hidden attractors with infinite equilibrium points. The first chaotic hidden attractor with stable equilibrium points was found in a generalized Chua system.[11] Hereafter, different chaotic systems[12–14] and hyperchaotic systems[15–17] with stable equilibrium points were reported. A chaotic system without equilibrium points was presented by Wei in 2011.[18] In 2013, Jafari *et al.* developed 17 quadratic flows with no equilibria by a systematic search.[19] To explore whether chaotic systems without equilibrium points are really hidden, Pham *et al.*, in 2014, investigated the hidden chaotic systems with no equilibrium point by starting the trajectory in the neighborhood of complex fixed-points.[20] They came to the conclusion that the chaotic systems with no equilibrium point are really hidden. In recent years, many hidden attractor systems without equilibrium points but with rich dynamical characteristics[21–23] were reported. In 2013, Jafari and Sprott introduced the concept that chaotic systems with line equilibrium points (infinite equilibrium points) can be classified as hidden attractor chaotic systems.[24] It also motivated researchers to investigate hidden attractor chaotic systems with infinite equilibrium points and rich dynamical characteristics.[25–27]

Recently, much attention has been paid to multiscroll hidden attractor chaotic systems that do not satisfy the Shilnikov criteria. In 2016, Jafari *et al.* reported a multiscroll chaotic system without equilibrium points by introducing a sine function into the Sprott A system.[28] In the same year, Hu *et al.* constructed a multiscroll chaotic system without equilibrium points based on an improved Sprott A system by introducing a nonlinear function composed of a sine function, a sign function, and a state variable.[29] The next year, Hu *et al.* used a memristor and a sine function to implement a 5-dimensional multiscroll chaotic system without equilibrium points.[30] Based on a multiple piecewise linear function, Escalante-González *et al.* proposed a multiscroll chaotic system without equilibrium points.[31] And they explored the mechanism of how the no equilibrium chaotic system generates multiscroll chaotic attractors.

Obviously, the multiscroll hidden attractor systems reported above mainly focused on systems without equilibrium points. It is also of great significance to study multiscroll chaotic systems with stable equilibrium points and infinite equilibrium points. Up to now, multiscroll chaotic attractors with stable equilibrium points have not been reported. In this paper, a multiscroll hidden attractor chaotic system is constructed by introducing a nonlinear function with multiple breakpoints. A notable feature of the novel system is that there are two equilibrium points of the system; the number of scrolls can be increased by adding breakpoints of the nonlinear function. Moreover, the two equilibrium points of the novel system are stable node-foci equilibrium points, that is to say, the novel multiscroll chaotic attractors are hidden attractors with stable equilibrium points.

The rest of this paper is organized as follows. The mathematical model of the novel system is presented in Sec. II. In Sec. III, the dynamical behaviors of the novel system are studied numerically.

TABLE I. Parameters of $f(z)$ and corresponding scroll numbers.

	Parameters of $f(z)$	Scroll numbers
Case 1	$E_1 = 0.3$, $N = 1$, $m_0 = -1$, and $m_1 = 1$	2×2 scrolls
Case 2	$E_1 = 0.3$, $N = 3$, $m_0 = m_2 = -1$, and $m_1 = m_3 = 1$	2×4 scrolls
Case 3	$E_1 = 0.3$, $N = 5$, $m_0 = m_2 = m_4 = -1$, and $m_1 = m_3 = m_5 = 1$	2×6 scrolls
Case 4	$E_1 = 0.3$, $N = 7$, $m_0 = m_2 = m_4 = m_6 = -1$, and $m_1 = m_3 = m_5 = m_7 = 1$	2×8 scrolls

A corresponding circuit for the implementation of the novel system is designed in Sec. IV. Finally, Sec. V concludes the paper.

II. THE SYSTEM MODEL

In this section, we propose a multiscroll chaotic system. The state equation is

$$\begin{cases} \dot{x} = y - ax \\ \dot{y} = -2x + nxw^2 - bxy + 10yf(z), \\ \dot{z} = 1 - y^2 \\ \dot{w} = -x - w \end{cases} \tag{1}$$

where a, b, and n are constant coefficients of the system state equation; $f(z)$ is a piecewise linear function and its formulation is

$$f(z) = m_N z + 0.5 \sum_{n=1}^{N} (m_{n-1} - m_n)(|z + E_n| - |z - E_n|), \tag{2}$$

$$E_n = \left(1 + 2 \sum_{i=1}^{n-1} \frac{|m_0|}{|m_i|}\right) E_1, \tag{3}$$

where E_n $(n = 1, 2, 3, \ldots, N)$ is the breakpoint of the function $f(z)$ and m_n $(n = 1, 2, 3, \ldots, N)$ is the slope rate. Let us take $a = 0.1$, $b = 0.4$, and $n = 0.02$. The parameters of the piecewise linear function $f(z)$ and the corresponding number of scrolls are shown in Table I. Figure 1 displays the phase portraits in the y-z plane of different number of scrolls. According to the numerical simulation, we can decide that the system can generate multiscroll attractors when N is an odd number. However, when N is an even number, there is no chaotic motion.

III. DYNAMICS BEHAVIORS

In this section, we take Case 2 in Table I as an example to study the dynamical behaviors of the novel system. The dynamical characteristics of the novel system are analyzed using equilibrium points and stability, a cross section of the attraction basin, the spectrum of Lyapunov exponents, a bifurcation diagram, and Poincaré maps.

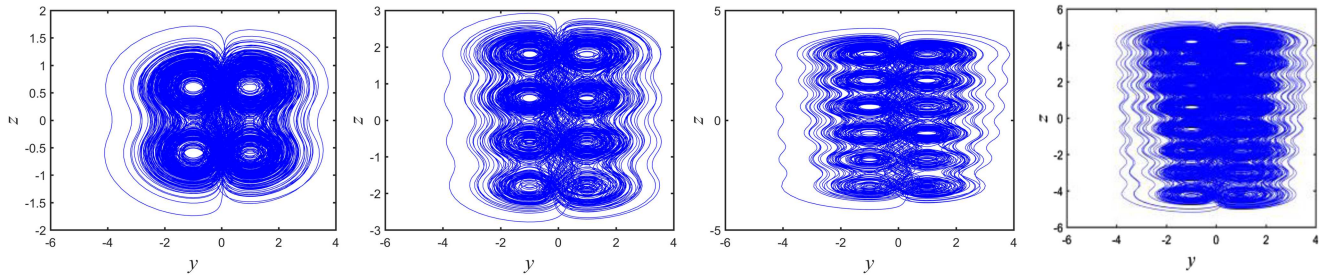

FIG. 1. Phase portraits in the *y*-*z* plane of (a) 2 × 2 scrolls, (b) 2 × 4 scrolls, (c) 2 × 6 scrolls, and (d) 2 × 8 scrolls.

A. Equilibrium points and stability analysis

The equilibrium points of system (1) can be obtained by solving the following equation:

$$\begin{cases} y - ax = 0 \\ -2x + nxw^2 - bxy + 10yf(z) = 0 \\ 1 - y^2 = 0 \\ -x - w = 0 \end{cases}. \tag{4}$$

From the first, third, and last equations of the above equation, we can easily derive $(x, y, w) = (1/a, 1, -1/a)$ and $(x, y, w) = (-1/a, -1, 1/a)$. To get the values of state variable z, we need to solve the following equations, which are derived by substituting the values of x, y, and w into Eq. (4):

$$\begin{cases} f(z) = \dfrac{1}{10}\left(\dfrac{2}{a} - n\left(\dfrac{1}{a}\right)^3 + \dfrac{b}{a}\right), \text{ when } (x, y, w) = \left(\dfrac{1}{a}, 1, -\dfrac{1}{a}\right), \\ f(z) = \dfrac{1}{10}\left(\dfrac{2}{a} - n\left(\dfrac{1}{a}\right)^3 - \dfrac{b}{a}\right), \text{ when } (x, y, w) = \left(-\dfrac{1}{a}, -1, \dfrac{1}{a}\right). \end{cases} \tag{5}$$

Considering the parameters, $a = 0.1$, $b = 0.4$, and $n = 0.02$, we can get $f(z) = 0.4$, when$(x, y, w) = (10, 1, -10)$, and $f(z) = -0.4$, when $(x, y, w) = (-10, 1, 10)$. Considering the Case 2 in Table I, the piecewise linear function $f(z)$ has parameters $E_1 = 0.3$, $N = 2$, $m_0 = m_2 = -1$, and $m_1 = m_3 = 1$. Figure 2 shows the diagram of function $f(z)$. It can be calculated that when $z = -E_3, z = -E_1$, and $z = E_2$, $f(z)$ equals to 0.3. When $z = -E_2$, $z = E_1$, and $z = E_3$, $f(z)$ equals to -0.3. From Fig. 2, we can determine that $f(z) = 0.4$ can be satisfied only when $z > E_3$, and $f(z) = -0.4$ can be satisfied only when $z < -E_3$. The expressions of $f(z)$ in these two parts are as follows:

$$\begin{cases} f(z) = z - 1.8, & \text{when } z > E_3, \\ f(z) = z + 1.8, & \text{when } z < -E_3. \end{cases} \tag{6}$$

We can get that when $z_1 = 2.2$, $f(z)$ equals to 0.4 and when $z_2 = -2.2$, $f(z)$ equals to -0.4. Thus, the two equilibrium points are $S_1(10, 1, 2.2, -10)$ and $S_2(-10, -1, -2.2, 10)$.

The Jacobian matrix of system (1) at equilibrium can be expressed as

$$J(S) = \begin{bmatrix} -a & 1 & 0 & 0 \\ -2 + nw^2 - by & -bx + 10f(z) & 10y & 2nxw \\ 0 & -2y & 0 & 0 \\ -1 & 0 & 0 & -1 \end{bmatrix}\Bigg|_S. \tag{7}$$

Substituting S_1 (10, 1, 2.2, −10) and $S_2(-10, -1, -2.2, 10)$ in the above equation, we have

$$J(S_1) = \begin{bmatrix} -0.1 & 1 & 0 & 0 \\ -0.4 & 0 & 10 & -4 \\ 0 & -2 & 0 & 0 \\ -1 & 0 & 0 & -1 \end{bmatrix} \tag{8}$$

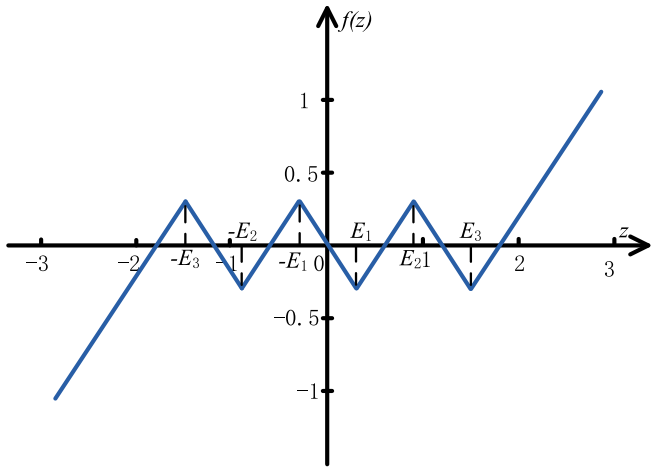

FIG. 2. Graph of the piecewise linear function $f(z)$ with $E_1 = 0.3$, $N = 3$, $m_0 = m_2 = -1$, and $m_1 = m_3 = 1$.

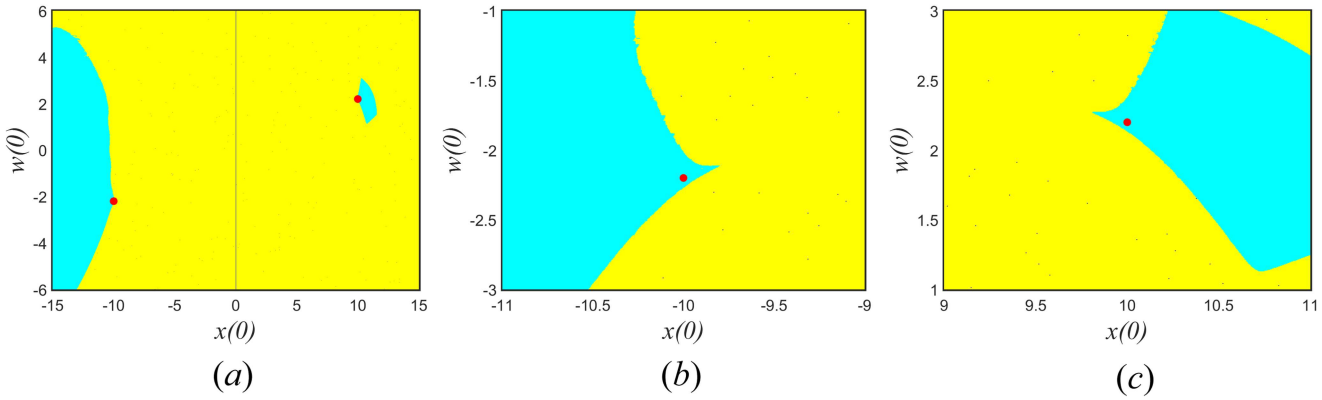

FIG. 3. Attraction basin of 2 × 4 scroll attractors (a) cross section passing through S_1 and S_2, (b) zooming in around S_1, and (c) zooming in around S_2.

and

$$J(S_2) = \begin{bmatrix} -0.1 & 1 & 0 & 0 \\ 0.4 & 0 & -10 & -4 \\ 0 & 2 & 0 & 0 \\ -1 & 0 & 0 & -1 \end{bmatrix}. \quad (9)$$

The characteristic roots of system (1) at equilibrium point S_1 are $\lambda_1 = -0.126$, $\lambda_2 = -0.7823$, and $\lambda_{3,4} = -0.0956 \pm 4.4965i$, and the characteristic roots at equilibrium point S_2 are $\lambda_1 = -0.1334$, $\lambda_2 = -0.7718$, and $\lambda_{3,4} = -0.0974 \pm 4.4058i$. In this case, both equilibrium points S_1 and S_2 are stable node-foci equilibrium points, which means the motions starting from the neighborhood of S_1 and S_2 will converge to them, respectively. However, the novel system generates chaotic attractors with 2 × 4 scrolls. This implies that the 2 × 4 scroll attractors are hidden attractors.

B. Attraction basin of the 2×4 scroll attractors

According to the definition of hidden attractors, if the attraction basin of chaotic attractors does not intersect with the open neighborhood of equilibrium points, the chaotic attractors can be called hidden attractors. To check whether the attraction basin intersects with small neighborhood of equilibrium points S_1 and S_2, a cross section plane $\{x, y = 0.1x, w = -x, z\}$ is selected to pass through the two stable equilibrium points. Figure 3(a) shows the attraction basin passing through the two stable equilibrium points S_1 and S_2 represented by red dots. Figures 3(b) and 3(c) display the enlarged regions around the equilibrium points S_1 and S_2, respectively. The attraction basin of chaotic attractors is indicated by yellow region; the cyan regions represent that the motion starting from these initial state regions will converge to the stable equilibrium points. It can be seen from Figs. 3(b) and 3(c) that the attraction basins of chaotic attractors do not intersect with the two stable equilibrium points. Thus, we can identify the attractors as hidden attractors.

Figure 4(a) displays the 3D view of the 2 × 4 scroll hidden attractors. Figure 4(b) shows the time domain wave of state variable z in 1×10^6 s. As can be seen from Fig. 4(b), the chaotic motion lasts for a long time, which means the hidden attractors do not have transitory behaviors.

C. Equilibrium points and stability of other cases

The equilibrium points of other cases in Table I can be obtained by the same analysis method. The two equilibrium points of Case 1 are S_1 (10, 1, 1, −10) and S_2 (−10, −1, −1, 10). The two equilibrium points of Case 3 are S_1 (10, 1, 3.4, −10) and S_2 (−10, −1, −3.4, 10).

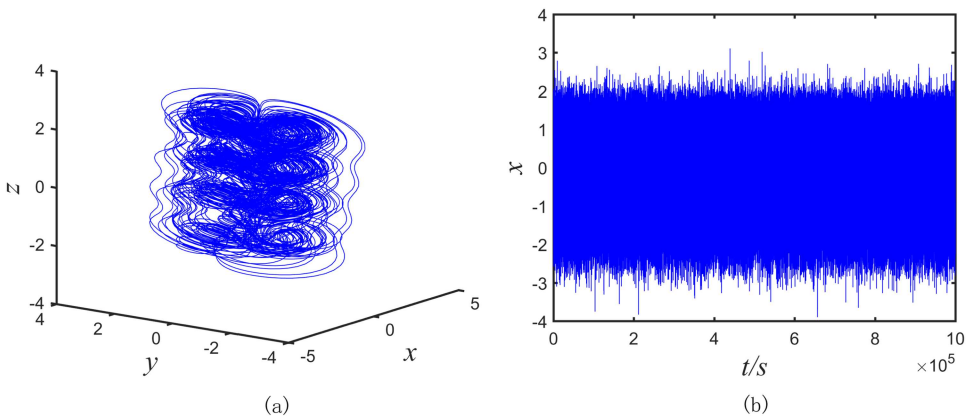

FIG. 4. (a) 3D view (*x*-*y*-*z*) of 2 × 4 scroll attractors; and (b) time domain wave of state variable z in 1×10^6 s.

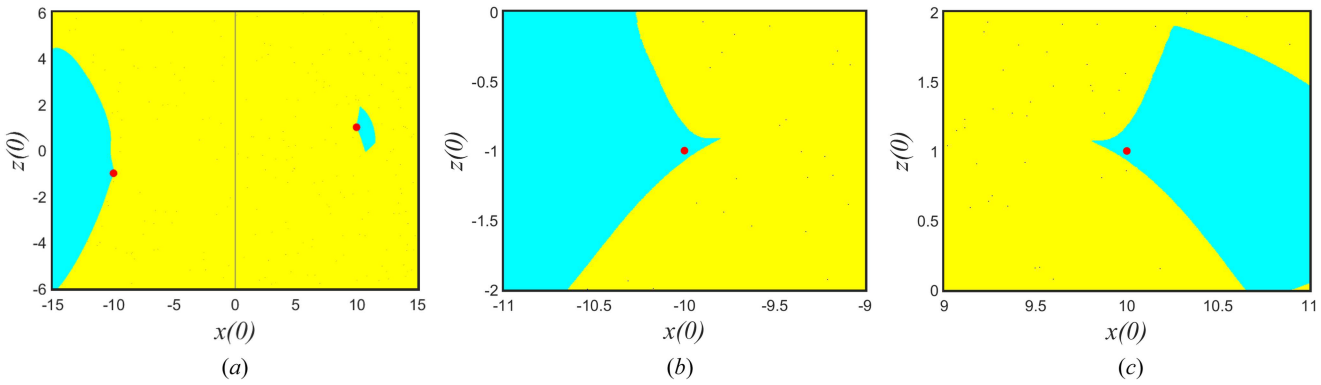

FIG. 5. Attraction basin of 2 × 2 scroll attractors (a) cross section passing through S_1 and S_2, (b) zooming in around S_1, and (c) zooming in around S_2.

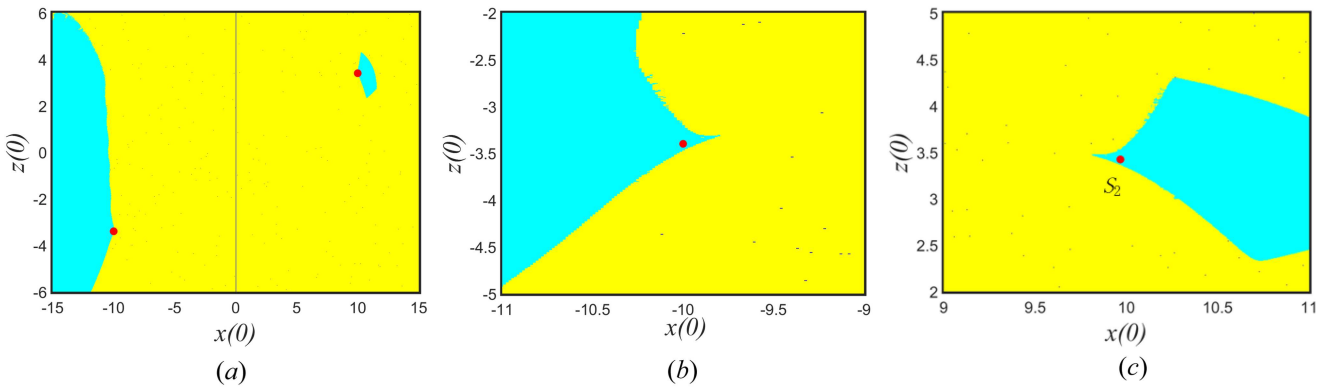

FIG. 6. Attraction basin of 2 × 6 scroll attractors (a) cross section passing through S_1 and S_2, (b) zooming in around S_1, and (c) zooming in around S_2.

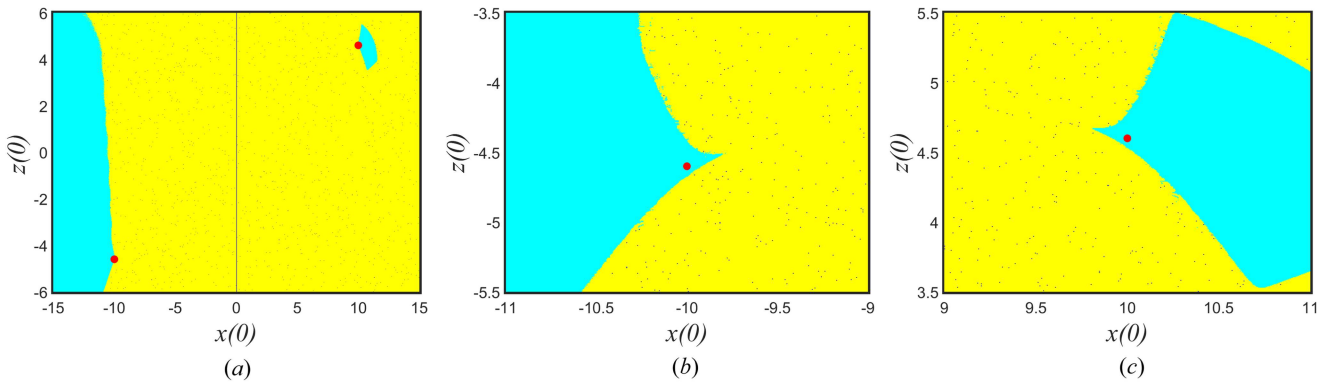

FIG. 7. Attraction basin of 2 × 8 scroll attractors (a) cross section passing through S_1 and S_2, (b) zooming in around S_1, and (c) zooming in around S_2.

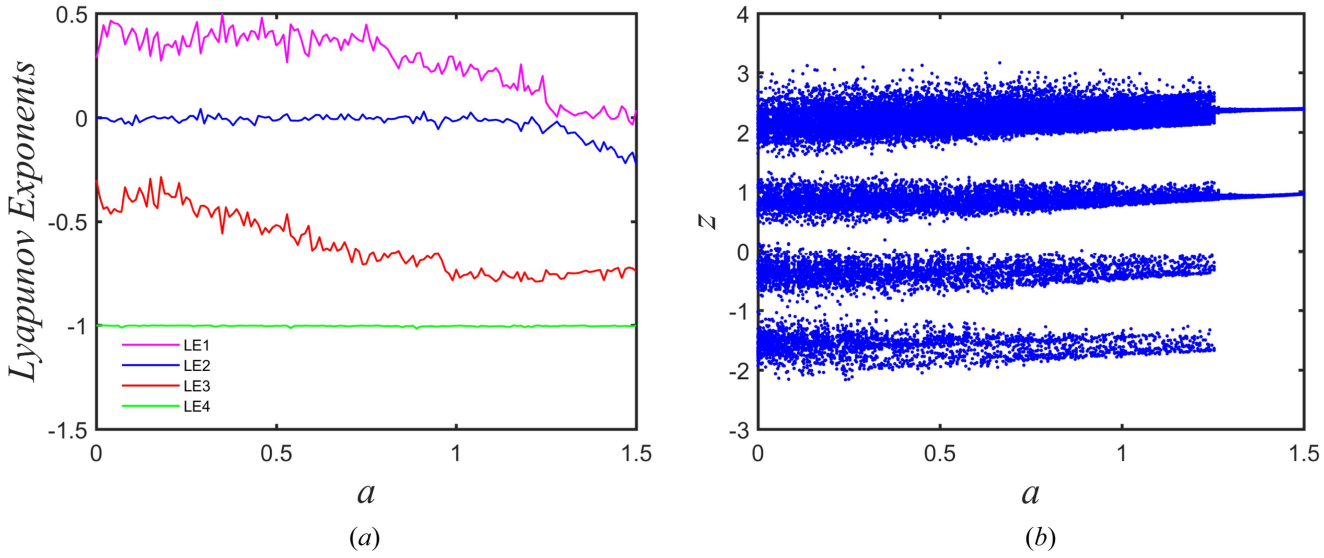

FIG. 8. (a) Spectrum of Lyapunov exponents changing *a* from 0 to 1.5; and (b) the corresponding bifurcation diagram of state variable *z*.

And the two equilibrium points of Case 4 are S_1 (10, 1, 4.6, −10) and S_2 (−10, −1, −4.6, 10). From Eq. (7), we can see that the value of state variable z has no effect on the eigenvalues of the Jacobian matrix. The eigenvalues of all cases are $\lambda_1 = -0.126$, $\lambda_2 = -0.7823$, and $\lambda_{3,4} = -0.0956 \pm 4.4965i$ at equilibrium point S_1, and $\lambda_1 = -0.1334$, $\lambda_2 = -0.7718$, and $\lambda_{3,4} = -0.0974 \pm 4.4058i$ at equilibrium point S_2. That is to say, all the cases in Table I are hidden attractors.

To further confirm these hidden attractors, we display the attraction basin of Case 1 in Fig. 5, the attraction basin of Case 3 in Fig. 6, and the attraction basin of Case 4 in Fig. 7. As can be seen in Figs. 5–7, the attraction basins of chaotic attractors, which are indicated by yellow region, do not intersect with any equilibrium points. Thus, we can determine these Cases as hidden attractors from the figures.

D. Lyapunov exponent spectra and bifurcation diagram

For further investigating the dynamics of system (1), the controlled parameter a is changed from 0 to 1.5, while fixing the other parameters $b = 0.4$, $n = 0.02$, $E_1 = 0.3$, $N = 3$, $m_0 = m_2 = -1$, and $m_1 = m_3 = 1$. The corresponding spectrum of Lyapunov exponents is shown in Fig. 8(a), and the bifurcation diagram of state variable z is shown in Fig. 8(b). According to the spectrum of Lyapunov exponents, when $a \in [0, 1.28)$, the maximum Lyapunov exponent is positive, indicating the system is chaotic in this parameter region, and when $a \in [1.28, 1.5]$, the maximum Lyapunov exponent equals to zero, indicating the system is periodic. The bifurcation of state variable z matches the spectrum of Lyapunov exponents very well.

E. Poincaré map

Figure 9 shows the Poincaré map diagram of the 2 × 4 scroll attractors. The Poincaré map of system (1) in *y-z*, *x-z*, *x-y*, and *x-w* planes are, respectively, shown in Figs. 9(a)–9(d). As can be seen in Fig. 9, the Poincaré maps of the system on different planes are a number of dense points, which indicate that the system has the characteristics of bifurcation and foldability of chaos.

IV. CIRCUIT IMPLEMENTATION

In this part, a circuit that can generate the 2 × 4 scroll hidden attractors is designed. And the hardware circuit is implemented by using TL082 op-amps. All the multipliers are selected, AD633JN, whose voltage gain is 0.1. The supply voltages of the circuit elements are ±15 V. The implementation circuit is shown in Fig. 10.

The voltage across the capacitors V_{c1}, V_{c2}, V_{c3}, and V_{c4} represents the variable values x, y, z, and w. The differential function can be changed as

$$\begin{cases} C_1 \dfrac{dx}{dt} = \dfrac{1}{R_1}x - \dfrac{1}{R_2}y \\ C_2 \dfrac{dy}{dt} = \dfrac{1}{R_3}x + \dfrac{1}{R_4}xy + \dfrac{1}{R_5}yf(z) - \dfrac{0.01}{R_6}xw^2 \\ C_3 \dfrac{dz}{dt} = \dfrac{1}{R_7}V_1 + \dfrac{0.1}{R_8}y^2 \\ C_4 \dfrac{dw}{dt} = \dfrac{1}{R_9}x + \dfrac{1}{R_{10}}z \end{cases}. \quad (10)$$

The values of capacitors are fixed as $C_1 = C_2 = C_3 = C_4 = 10$ nF. Based on the parameters of the 2 × 4 scroll attractors, the values of resistors are set as $R_1 = 1$ MΩ, $R_2 = R_3 = R_4 = R_7 = R_9 = R_{10} = 100$ kΩ, $R_5 = R_8 = 10$ kΩ, and $R_6 = 2$ MΩ. The piecewise linear function $f(z)$ is implemented by saturation function circuits. And the saturated

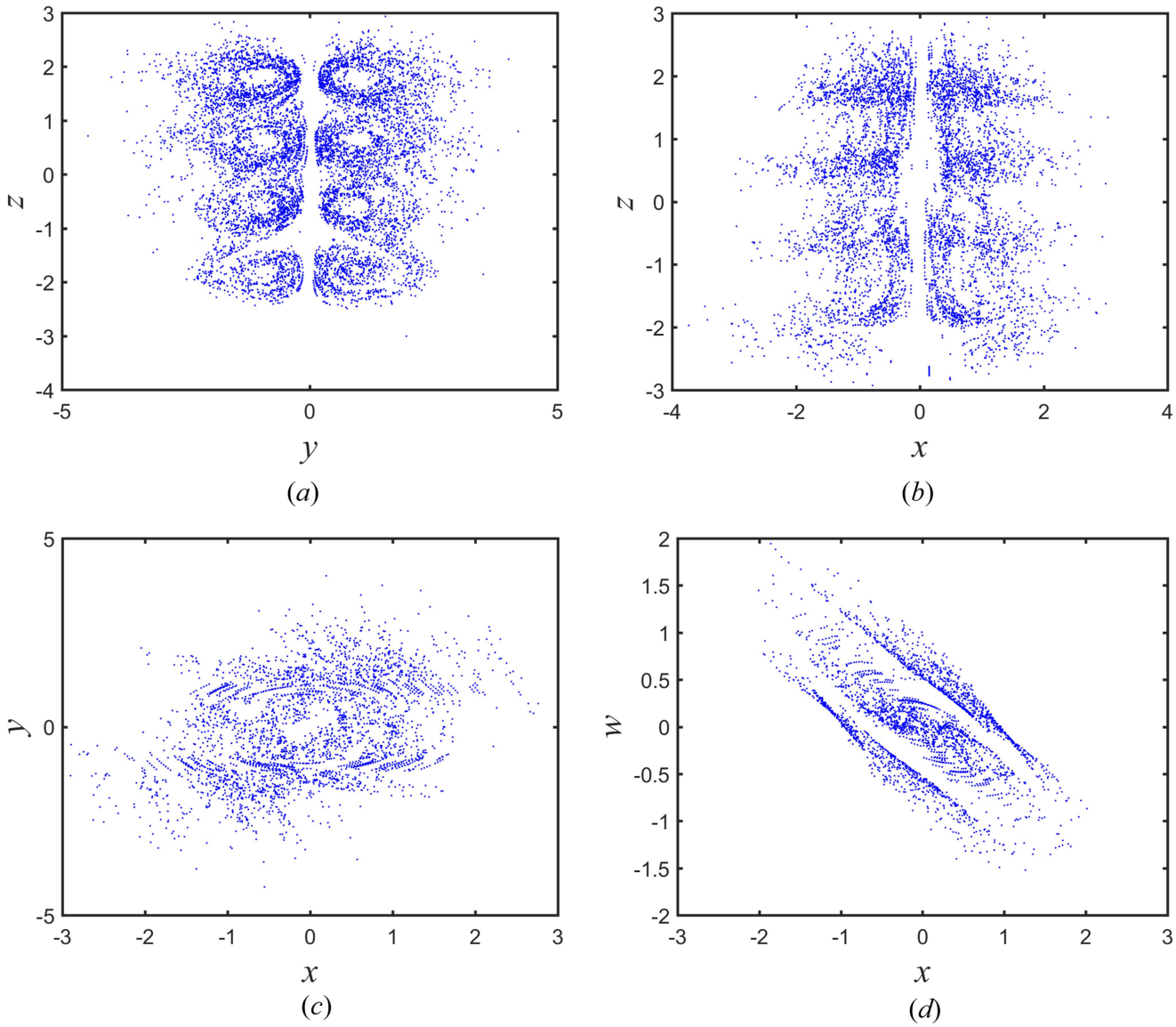

FIG. 9. Poincaré map in the (a) *y*-*z* plane, (b) *x*-*z* plane, (c) *x*-*y* plane, and (d) *x*-*w* plane.

output voltage of TL082 is $V_{\text{sat}} = \pm 13.5$ V. The math relationships of circuit parameters and the corresponding parameters of function $f(z)$ can be expressed as follows:

$$\begin{aligned} E_1 &= \frac{R_a}{R_b}|V_{sat}|, \\ E_2 &= \left(1 + \frac{R_a}{R_b}\right) V_2 - \frac{R_a}{R_b}|V_{sat}|, \\ E_3 &= \left(1 + \frac{R_a}{R_b}\right) V_2 + \frac{R_a}{R_b}|V_{sat}|, \end{aligned} \tag{11}$$

$$\begin{aligned} m_0 = m_2 &= -\frac{R_b}{R_a R_c}, \\ m_1 = m_3 &= \frac{R_b}{R_a R_c}. \end{aligned}$$

Set the value of resistor as $R_b = 1350\,\text{k}\Omega$. According to the parameter settings of piecewise linear function $f(z)$, the values of other resistors and DC voltages, as shown in Fig. 10(b), can be calculated as $R_a = 30\,\text{k}\Omega$, $R_c = 45\,\text{k}\Omega$, $R_{11} = 20\,\text{k}\Omega$, $V2 = 1.1739$ V, and $V3 = -1.1739$ V. Figure 11 shows the phase portraits generated by the hardware experiment and software simulation of NI Multisim.

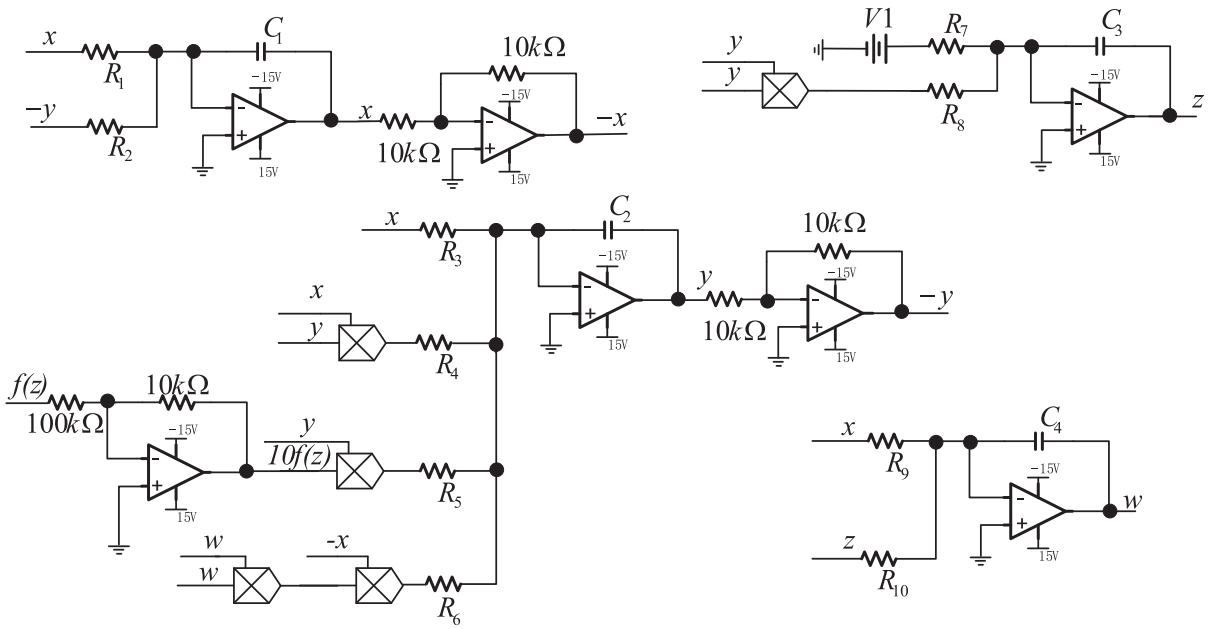

(a)

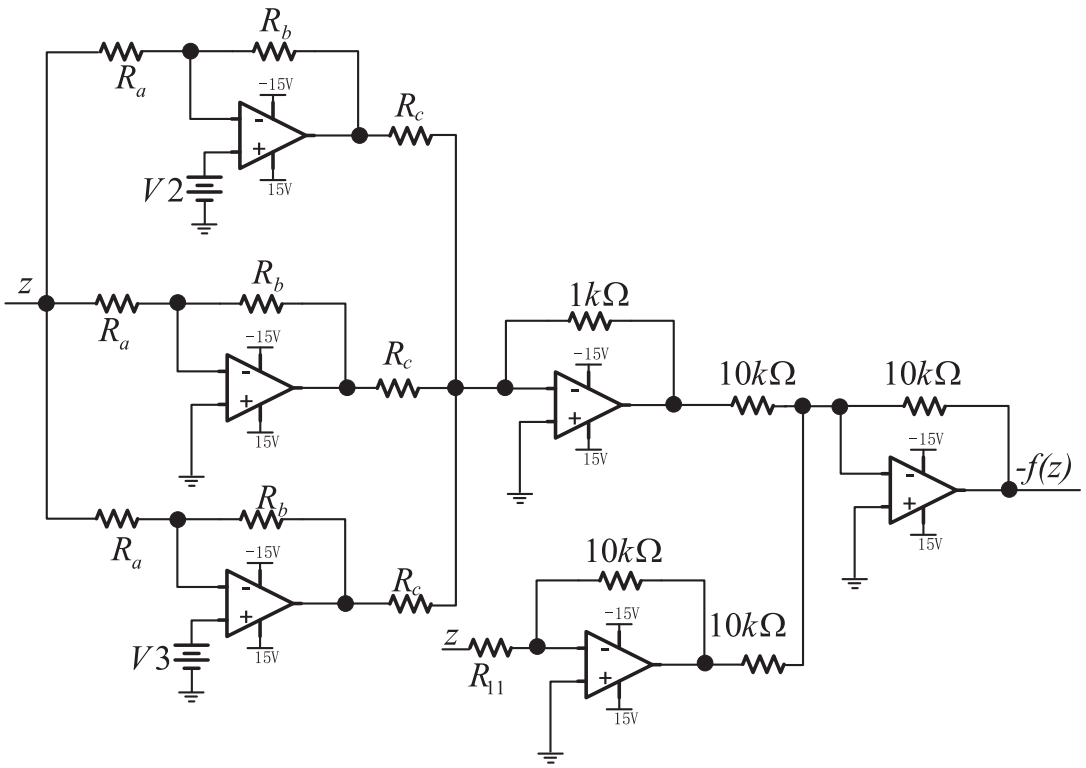

(b)

FIG. 10. Circuit models for implementing 2 × 4 scroll hidden attractors. (a) Fundamental circuit for a four-dimensional system. (b) Circuit for generating the piecewise linear function $f(z)$.

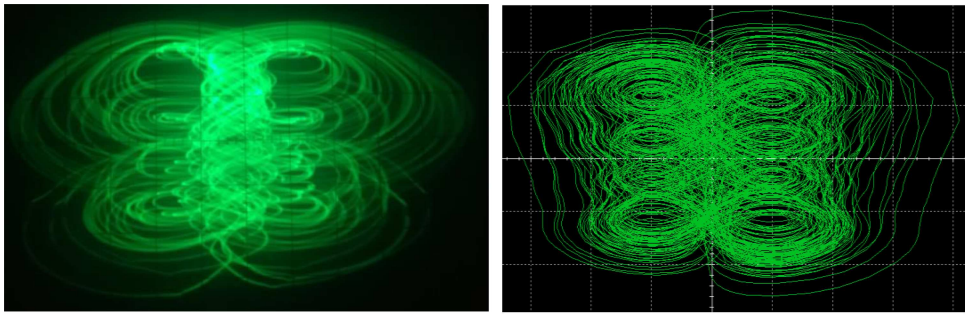

(a) (b)

FIG. 11. Phase portraits of 2 × 4 scroll hidden attractors (a) in the *y-z* plane implementation by hardware; and (b) in the *y-z* plane simulated by NI Multisim software.

V. CONCLUSION

In this paper, we propose a multiscroll chaotic system. The novel system has only two stable node-foci equilibrium points. The number of scrolls can be increased by adding breakpoints of the piecewise linear function. The multiscroll hidden attractors are verified by the attraction basin. Performances of the hidden attractors are investigated by phase portraits, the spectrum of Lyapunov exponents, the bifurcation diagram, and the Poincaré map. The hardware experiment of the proposed system is carried out. It is believed that the proposed novel system will contribute to the development of the theoretical study of a multiscroll hidden attractor.

ACKNOWLEDGMENTS

This work is supported by the National Natural Science Foundation of China (NNSFC) (Grant No. 61571185).

REFERENCES

[1]K. Li, M. Zhao, and X. Fu, "Projective synchronization of driving–response systems and its application to secure communication," IEEE Trans. Circuits Syst. **56**(10), 2280–2291 (2009).
[2]Y. Li, C. Wang, and H. Chen, "A hyper-chaos-based image encryption algorithm using pixel-level permutation and bit-level permutation," Opt. Lasers Eng. **90**, 238–246 (2017).
[3]Q. Yin and C. Wang, "A new chaotic image encryption scheme using breadth-first search and dynamic diffusion," Int. J. Bifurcat. Chaos **28**(04), 1850047 (2018).
[4]J. A. Suykens and L. O. Chua, "n-double scroll hypercubes in 1-D CNNs," Int. J. Bifurcat. Chaos **07**(08), 1873–1885 (1997).
[5]L. P. Shilnikov, "A case of the existence of a denumerable set of periodic motions," Sov. Math. Dokl. **6**, 163–166 (1965).
[6]J. A. Suykens and J. Vandewalle, "Generation of n-double scrolls (n= 1, 2, 3, 4,…)," IEEE Trans. Circuits Syst. I **40**(11), 861–867 (1993).
[7]C. Wang, H. Xia, and L. Zhou, "A memristive hyperchaotic multiscroll Jerk system with controllable scroll numbers," Int. J. Bifurcat. Chaos **27**(06), 1750091 (2017).
[8]X. Zhang and C. Wang, "A novel multi-attractor period multi-scroll chaotic integrated circuit based on CMOS wide adjustable CCCII," IEEE Access **7**, 16336–16350 (2019).
[9]C. Wang, X. Liu, and H. Xia, "Multi-piecewise quadratic nonlinearity memristor and its 2N-scroll and 2N+1-scroll chaotic attractors system," Chaos **27**(3), 033114 (2017).
[10]G. A. Leonov, N. V. Kuznetsov, and V. I. Vagaitesev, "Localization of hidden Chua's attractors," Phys. Lett. A **375**(23), 2230–2233 (2011).
[11]N. V. Kuznetsov, G. A. Leonov, and V. I. Vagaitsev, "Analytical numerical method for attractor localization of generalized Chua's system," IFAC Proc. **43**(11), 29 (2010).
[12]Q. Yang, Z. Wei, and G. R. Chen, "An unusual 3D autonomous quadratic chaotic system with two stable node-foci," Int. J. Bifurcat. Chaos **20**(04), 1061–1083 (2010).
[13]W. C. Wei and Q. G. Yang, "Dynamical analysis of the generalized Sprott C system with only two stable equilibria," Nonlinear Dyn. **68**(4), 543–554 (2012).
[14]S. Cang, Y. Li, R. Zhang, and Z. Wang, "Hidden and self-excited coexisting attractors in a Lorenz-like system with two equilibrium points," Nonlinear Dyn. **95**(1), 381–390 (2019).
[15]Z. Wei and W. Zhang, "Hidden hyperchaotic attractors in a modified Lorenz–Stenflo system with only one stable equilibrium," Int. J. Bifurcat. Chaos **24**(10), 1450127 (2014).
[16]Z. Wei, I. Moroz, J. C. Sprott, A. Akgul, and W. Zhang, "Hidden hyperchaos and electronic circuit application in a 5D self-exciting homopolar disc dynamo," Chaos **27**(3), 033101 (2017).
[17]Z. Wei, P. Yu, W. Zhang, and M. Yao, "Study of hidden attractors, multiple limit cycles from Hopf bifurcation and boundedness of motion in the generalized hyperchaotic Rabinovich system," Nonlinear Dyn. **82**(1–2), 131–141 (2015).
[18]Z. Wei, "Dynamical behaviors of a chaotic system with no equilibria," Phys. Lett. A **376**(2), 102–108 (2011).
[19]S. Jafari, J. C. Sprott, and S. M. R. H. Golpayegani, "Elementary quadratic chaotic flows with no equilibria," Phys. Lett. A **377**(9), 699–702 (2013).
[20]V. T. Pham, S. Jafari, C. Volos, X. Wang, and S. M. R. H. Golpayegani, "Is that really hidden? The presence of complex fixed-points in chaotic flows with no equilibria," Int. J. Bifurcat. Chaos **24**(11), 1450146 (2015).
[21]L. Zhou, C. Wang, and L. Zhou, "A novel no-equilibrium hyperchaotic multiwing system via introducing memristor," Int. J. Circ. Theor. Appl. **46**(1), 84–98 (2018).
[22]S. Zhang, Y. Zeng, Z. Li, M. Wang, and L. Xiong, "Generating one to four-wing hidden attractors in a novel 4d no-equilibrium chaotic system with extreme multistability," Chaos **28**(1), 013113 (2018).
[23]B. C. Bao, H. Bao, N. Wang, M. Chen, and Q. Xu, "Hidden extreme multistability in memristive hyperchaotic system," Chaos Solitons Fractals **94**, 102–111 (2017).
[24]S. Jafari and J. C. Sprott, "Simple chaotic flows with a line equilibrium," Chaos Solitons Fractals **57**, 79–84 (2013).
[25]L. Zhou, C. Wang, and L. Zhou, "Generating hyperchaotic multi-wing attractor in a 4D memristive circuit," Nonlinear Dyn. **85**(4), 2653–2663 (2016).
[26]Q. Tan, Y. Zeng, and Z. Li, "A simple inductor-free memristive circuit with three line equilibria," Nonlinear Dyn. **94**(3), 1585–1602 (2018).
[27]B. Bao, T. Jiang, Q. Xu, M. Chen, H. Wu, and Y. Hu, "Coexisting infinitely many attractors in active band-pass filter-based memristive circuit," Nonlinear Dyn. **86**(3), 1711–1723 (2016).
[28]S. Jafari, V. T. Pham, and T. Kapitaniak, "Multiscroll chaotic sea obtained from a simple 3D system without equilibrium," Int. J. Bifurcat. Chaos **26**(02), 1650031 (2016).
[29]X. Hu, C. Liu, L. Liu, J. Ni, and S. Li, "Multi-scroll hidden attractors in improved Sprott A system," Nonlinear Dyn. **86**(3), 1725–1734 (2016).
[30]X. Hu, C. Liu, L. Liu, Y. Yao, and G. Zheng, "Multi-scroll hidden attractors and multi-wing hidden attractors in a 5-dimensional memristive system," Chin. Phys. B **26**(11), 110502 (2017).
[31]R. D. J. Escalante-González, E. Campos-Cantón, and M. Nicol, "Generation of multi-scroll attractors without equilibria via piecewise linear systems," Chaos **27**(5), 053109 (2017).